TITLE:

Poly(3-hydroxybutyrate-co-3-hydroxyhexanoate) microcellular foams using a melt memory effect as bubble nucleation sites

AUTHOR(S):

Lee, Jisuk; Moriyama, Kenta; Hikima, Yuta; Ohshima, Masahiro

京都大学学術情報リポジトリ
KURENAI 紅
Kyoto University Research Information Repository

京都大学
KYOTO UNIVERSITY

KURENAI 紅
京都大学学術情報リポジトリ
Kyoto University Research Information Repository

RESEARCH ARTICLE

JOURNAL OF
Applied Polymer SCIENCE WILEY

Poly(3-hydroxybutyrate-co-3-hydroxyhexanoate) microcellular foams using a melt memory effect as bubble nucleation sites

Jisuk Lee | **Kenta Moriyama** | **Yuta Hikima** | **Masahiro Ohshima**

Department of Chemical Engineering, Kyoto University, Kyoto, Japan

Correspondence
Jisuk Lee, Department of Chemical Engineering, Kyoto University, Kyoto 615-8510, Japan.
Email: jskmlee@gmail.com

Abstract

Poly(3-hydroxybutyrate-co-3-hydroxyhexanoate) (PHBH) foams were prepared by a foam injection molding (FIM) process using nitrogen (N_2) as a physical blowing agent. PHBH is a marine degradable polymer known for its heat treatment weakness. Gel permeation chromatography and rheological measurements showed that the molecular weight was reduced when the polymer was processed at a temperature higher than 160°C; however, it had a prominent melt memory of crystallization at a temperature lower than 170°C. The melt memory effect increased the crystallization temperature and provided crystal nucleation sites, which became bubble nucleation sites in the foaming process. Microcellular foams, whose cell size is smaller than 30 μm and cell density is higher than 3×10^8 cells cm^{-3}, were prepared using the melt memory effect while suppressing the thermal decomposition by tuning the injected polymer's temperature (melting temperature) and the core-back timing. The mechanical properties of the resulting foams were evaluated, indicating that a high ductility PHBH microcellular foam was obtained at a melting temperature of 150°C.

KEYWORDS
biodegradable, crystallization, foams, mechanical properties, rheology

1 | INTRODUCTION

Natural resources are receiving much attention due to increasing environmental concerns. Various biobased and biodegradable polymers have been developed and applied to reduce environmental burdens. Among biobased and biodegradable polymers, poly(3-hydroxybutyrate-co-3-hydroxyhexanoate) (PHBH) is a biodegradable polymer made from genetically engineered bacteria, and it is known to degrade in the ocean and soil.[1] PHBH is a type of polyhydroxyalkanoate (PHA), and it is a copolymer of polyhydroxybutyrate (PHB) and polyhydroxyhexanoate (PHH).[2,3] PHB has high crystallinity and is brittle. In addition, the melting point and decomposition temperature are close, giving it a narrow temperature range for feasible processing. To overcome this issue, comonomers such as PHH were introduced to PHB.[4] The higher the ratio of PHH in PHBH is, the lower the crystallinity and crystallization rate, resulting in higher ductility, lower modulus, and strength.[4–6] Due to these properties of PHBH, PHBH

京都大学
KYOTO UNIVERSITY
LEE ET AL.

A Self-archived copy in
Kyoto University Research Information Repository
https://repository.kulib.kyoto-u.ac.jp

KURENAI 紅
京都大学学術情報リポジトリ
Kyoto University Research Information Repository

Applied Polymer—WILEY⎤ 2 of 11

exhibits a broader processing window with better thermal stability than other PHAs. However, the thermal treatment weakness and slow crystallization rate of PHBH need further improvements to expand its applications, requiring short cycle times and easy processability while maintaining its green nature. Several studies have challenged this issue, focusing on enhancing the crystallization rate by adding additives or accelerators.[7,8]

Polymer foaming has been considered a solution for reducing plastic consumption while ensuring sufficient plastic products for our society. In addition to weight reduction, polymer foams have characteristics such as sound insulation, heat insulation, and impact resistance.[9,10] In particular, microcellular foaming has been receiving much attention for several decades as a green polymer processing technology. It is usually conducted using nitrogen (N_2) as a physical blowing agent (PBA), an eco-friendly agent that reduces the environmental burden.[10] The cells of the microcellular foams are several tens of microns in diameter and 10^7–10^9 cells cm^{-3} in cell density.[11,12] Much research on the microcellular foaming of biodegradable polymers has been conducted. Most of them dealt with poly(lactide acid) (PLA)[13] and poly(butylene succinate) (PBS).[14] There is little research available on PHBH microcellular foams.

When foaming semicrystalline polymers, the nucleating crystals become a bubble nucleating agent in microcellular foaming.[12,15,16] PHBH is a semicrystalline polymer with slow crystallization but a prominent melt memory effect.[17–20] The melt memory effect is a phenomenon in which the polymer itself becomes a crystal nucleating agent and undergoes self-nucleation.[18,21] The melt memory is presumably the result of the residual orientation of chain segments of the molten polymer and small crystal fragments. Although various hypotheses exist for the origin of melt memory, the exact cause has not been elucidated and is still under investigation.

In this study, the microcellular foaming of PHBH was conducted using a recently developed foam injection molding process (RIC-Foam/SOFIT)[22,23] to observe whether the crystals or the melt memory effect could contribute to cell nucleation and lead to the formation of a fine cellular structure. The rheological measurement confirmed the viscosity reduction with increased polymer melting temperature and the exponential relationship between zero-shear viscosity and molecular weight. Thermal analysis revealed that the melt memory effect of PHBH occurred in the melting temperature range from 150 to 170°C. Based on these data of fundamental polymer properties, optimal foaming conditions of foam injection molding (FIM) were found to produce microcellular foam with higher ductility. The results will contribute to broadening the application of PHBH foams.

2 | EXPERIMENTAL

2.1 | Materials

PHBH with a $M_w \approx 450,000$ containing 6 mol% 3-HH (X131A) was provided by Kaneka Corp., Tokyo, Japan and used as received.

2.2 | Foam injection molding

A new type of foam injection molding (FIM) machine was developed with the cooperation of Kyoto University, Maxell Ltd. Co., and Japan Steel Works, Ltd. Co, named resilient and innovative foam injection molding (RIC-Foam).[22,23] The machine does not need any pumping or compressing gas systems to increase the PBA pressure and can perform foam processing with a low-gas delivery pressure (1–10 MPa), directly connecting the machine to a gas cylinder. A 35-tonnage-clamping force injection mold machine (J35AD-30H, Japan Steel Work Ltd.) was used with N_2 in this study. A cylindrical screw with a diameter of 20 mm and a 24 L/D ratio was used.

A core-back operation (precise mold opening) scheme was employed to enhance the foamability and control the cell size and density of the foams.[23] The difference between core-back and conventional FIM lies in an additional mold-opening operation. In the core-back FIM process, a part of the mold is quickly opened to expand the cavity volume. This mold opening operation initiates cell nucleation and growth by the rapid pressure drop and produces a fine cellular structure. In the experiments, the mold part was opened at a rate of 20 mm s^{-1}. The expansion ratio of foams was set to three by adjusting the core-back (mold opening) distance from a 1-mm initial cavity thickness (total 3 mm in foam thickness). The molding temperature was set to 30°C, and the cooling time was 60 s, which was relatively longer than the conventional cooling time. The nozzle and metering zones of the barrel of the injection molding machine, hereafter referred to as the melting temperature, were changed in the range from 150 to 190°C to observe the effect of the temperature of the injected polymer on its thermal degradation, cell structure and mechanical properties.

The mold has a rectangular mold cavity ($70 \times 50 \times 1$ mm^3) and contains two infrared temperature sensors and two pressure sensors to measure the polymer temperatures and pressures at different locations: one location was close to the inlet, and the other was at the flow end, as shown in Figure S1 in the Supporting Information. The detailed operation of the FIM with the mold-opening (core-back) operation can be found in our previous

---

Content:

TABLE 1 Processing condition

Parameter	Unit	Setpoint value
Blowing agent		N_2
Gas delivery pressure	MPa	7
Melting temperature	°C	150/160/170/180/190
Mold temperature	°C	30
Injection speed	mm s^{-1}	100
Holding pressure	MPa	20
Cooling time	s	60
Core-back distance	mm	2
Core-back velocity	mm s^{-1}	20

work.[11,12,24] The other processing parameters are summarized in Table 1.

2.3 | Cell structure characterization

The cell structure of PHBH foams was observed by a scanning electron microscope (SEM: Tiny-SEM Mighty-8, Technex Lab Co., Ltd., Japan). For SEM observation, a specimen was cut out from the center of the injection-molded products after cryogenically solidifying in liquid nitrogen. The observation was made parallel to the core-back direction, that is, the thickness direction of the foam. Before the SEM observation, the cross-sectional area was coated with carbon by a quick carbon coater (SC-701CT, Sanyu Electric Inc., Japan).

Cell density was calculated from the SEM images using ImageJ software (the National Institute of Health, USA). The formulas for cell density are given by Equation (1):

$$N_0 = \left(\frac{n}{A}\right)^{3/2} \times \phi \qquad (1)$$

where n is the number of cells in the selected area of the SEM image, A is the area of the image, and ϕ is the volume expansion ratio of the foamed sample.

2.4 | Rheology measurement

The rheological properties were measured using an ARES rheometer (TA Instruments, USA) with a parallel-plate device. The size of the disk-shaped specimens was 25 mm in diameter and 1.9 mm in thickness. The specimen was prepared by hot pressing pellets of the polymer. The heat treatment process involved maintaining the pellet at 160°C with 20 MPa compressive pressure for 3 min, then cooling the molten polymer to 30°C and annealing for 10 min. Frequency sweep tests were conducted at various temperatures with 0.1% strain by changing the strain rate frequency from 100 to 0.1 rad s^{-1}. Temperature sweep tests were also conducted to observe crystallization through the viscosity change. The measurement was carried out at a cooling rate of 10°C min^{-1} from several melting temperatures with a frequency of 10 rad s^{-1} and 0.1% strain after holding the designated melting temperature for 3 min. A time sweep test was used to identify the effect of melting temperature on thermal decomposition through viscosity reduction. The measurement was conducted at 10 rad s^{-1} frequency with 0.1% strain while maintaining a constant melting temperature. The specimen preparation of both tests was the same as that of the frequency sweep tests.

2.5 | Thermal analysis

Thermal analysis was conducted using a conventional differential scanning calorimeter (DSC) (DSC 7020, Hitachi High-Tech Science Corp., Japan). Approximately 5–7 mg specimens were used for the nonisothermal measurements. The specimens were prepared by cutting a piece from the center of the foam injection-molded product. Both heat and cooling curves were obtained by changing the temperature between −20°C and a specified melting temperature, that is, 150, 160, 170, 180, and 190°C, at 10°C min^{-1} heating and cooling rates in a nitrogen atmosphere. The melting temperature, T_m, and crystallization temperature, T_c, were calculated from the heating and cooling curves, respectively.

The crystallization behavior of the polymer injected into the mold cavity was characterized during the rapid cooling process using a chip-based fast-scanning calorimeter (FSC) (Flash DSC1, Mettler Toledo, USA). To simulate the heat treatment of the polymer injected into the mold cavity, a small piece of PHBH specimen was heated to one of five different melting temperatures, 150, 160, 170, 180, and 190°C, at a heating rate of 300°C s^{-1}, cooled to an isothermal crystallization temperature of 30°C at a cooling rate of 20°C s^{-1}, and held at the isothermal crystallization temperature for various annealing times, as shown in Figure S2. The cooling rate of 20°C s^{-1} was the average cooling rate of the injected polymer in the mold cavity. The specimen was prepared from PHBH pellets using a microtome (Nippon Optical Works Co., Ltd., Japan). The exothermic heat generated by the crystallization of PHBH at the isothermal crystallization temperature was too weak to be identified. Therefore, a discrete method[25] was employed to observe the evolution of crystallinity over time. The annealing time was changed from 0.1 to 1000 s. Just after annealing, the specimen was heated to the initial melting temperature at a heating rate of 300°C s^{-1} to obtain an endothermic curve, as shown in Figure S2. The crystallization behavior was calculated from the endothermic curve.
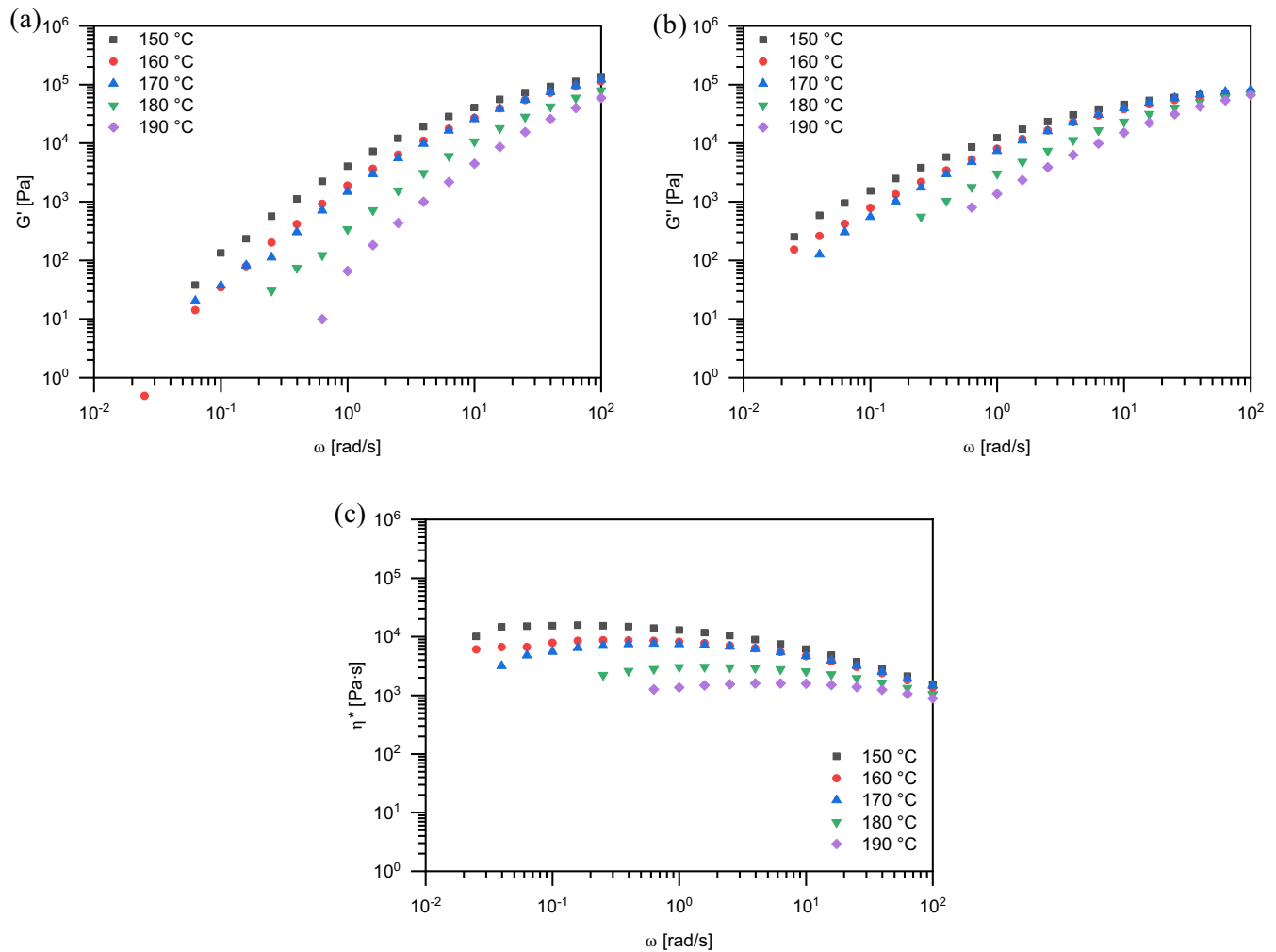
FIGURE 1 Frequency sweep test results at various temperatures; (a) storage modulus, (b) loss modulus and (c) complex viscosity. [Color figure can be viewed at wileyonlinelibrary.com]
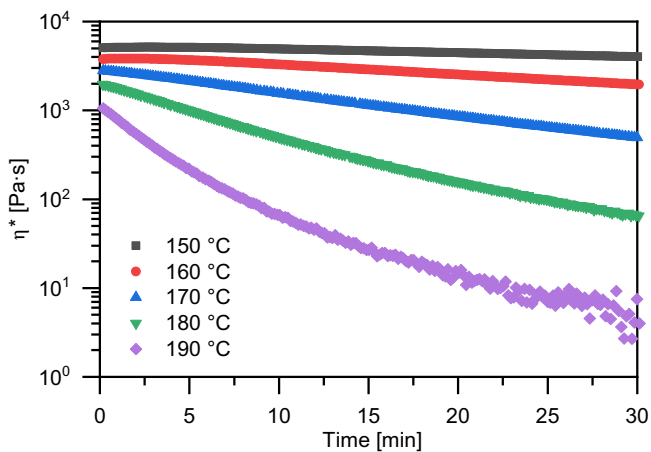

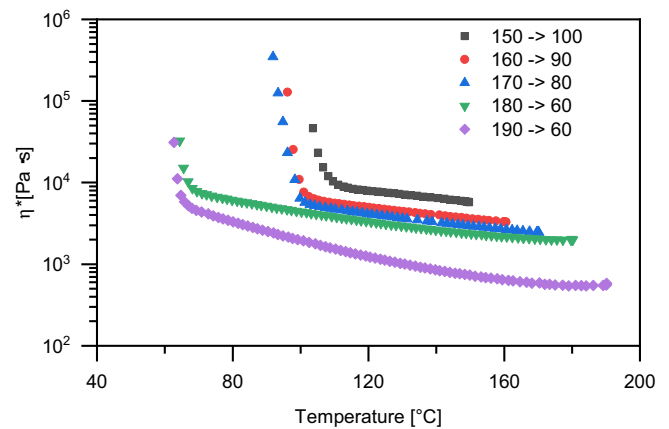**FIGURE 2** Results of the time sweeps tests at various temperatures. [Color figure can be viewed at wileyonlinelibrary.com]

FIGURE 3 Results of the temperature sweep tests at various melting temperatures. [Color figure can be viewed at wileyonlinelibrary.com]

2.6 │ Polarizing microscope observation of the crystal size with and without melt memory effect

To observe the melt memory effect on the crystal size of PHBH, separately from the molecular weight decomposition, rectangular-shaped specimens, 18 mm in length, 4 mm in width, and 2 mm in thickness, were prepared at 150, 160, 170, 180, and 190°C melting temperatures by hot pressing the pellets. The holding time on the hot pressing was adjusted so that the weight-average molecular weight ($\overline{M}_w$) of the specimens was approximately 200,000 g mol^{-1} despite the difference in the melt temperatures. After hot pressing, the specimens were cooled down and annealed at 40°C for 10 min to grow the crystals. Then, the hot-compressed specimen was cut to a thickness of 20 μm using a microtome (Nippon Optical Works Co., Ltd., Japan). A polarizing microscope (BX51-P, Olympus, Japan) was used to observe the crystal size of specimens to identify the effect of melting temperature, that is, the melt memory effect, on the crystal size.

2.7 │ Compression test

The compression tests of the resulting foams were conducted at room temperature with universal test equipment (Autograph AGS-1kN, Shimadzu, Japan). Cuboid-shaped specimens were prepared by cutting out the foam injection-molded products. The specimen size was
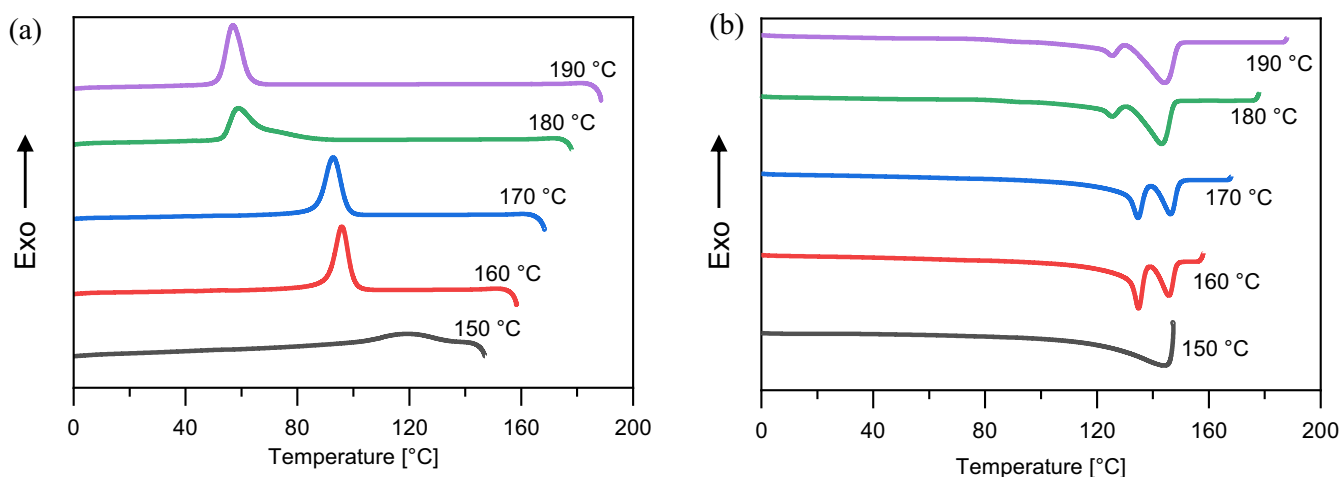

FIGURE 4 Differential thermal curves of PHBH during (a) first cooling and (b) second heating at a 10°C min^{-1} of cooling rate and heating rate. [Color figure can be viewed at wileyonlinelibrary.com]
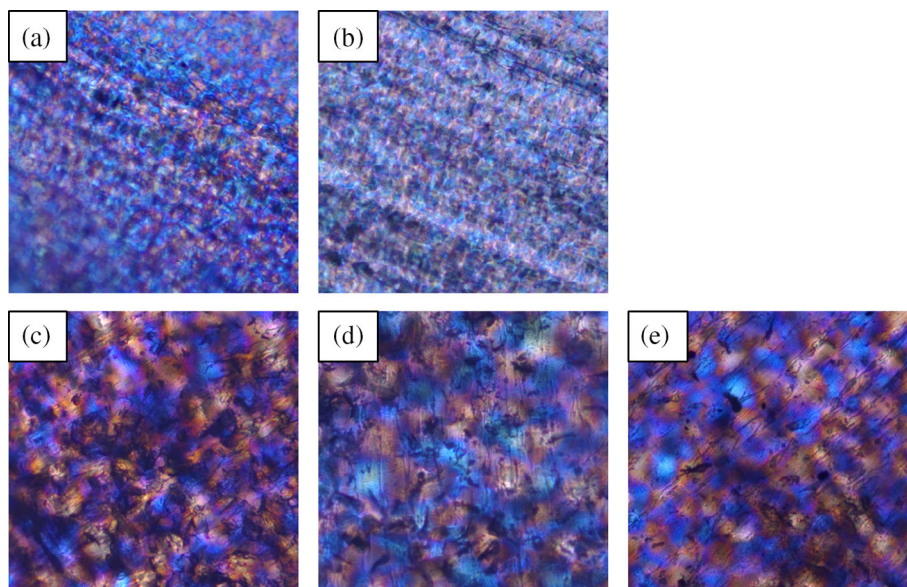

FIGURE 5 Polarizing microscope images of the PHBH specimens cooled at 40°C after being melted at the different melting temperatures; (a) 150°C, (b) 160°C, (c) 170°C, (d) 180°C and (e) 190°C. [Color figure can be viewed at wileyonlinelibrary.com]

50 mm in width, 50 mm in length, and 30 mm in thickness. The crosshead speed was set to 0.5 mm min^{-1}. All conditions followed ISO 844 and ISO 1923. The modulus of elasticity was calculated by Equation (2), averaging at least five samples' values:

$$E = \frac{\Delta\sigma}{\Delta\varepsilon} \quad (2)$$

where $\Delta\sigma$ is the change in compressive strength in a proportional section of the strain–stress curve, and $\Delta\varepsilon$ is the displacement in the elastic area.

2.8 | Open cell content measurement

The open cell content of foams was measured using a gas pycnometer (AccuPycII, Shimadzu, Japan). The specimen was cut out from the center of the foam-injection-molded product to 30 mm in height, 15 mm in width, and 3 mm in thickness. The open cell content was calculated by Equation (3):
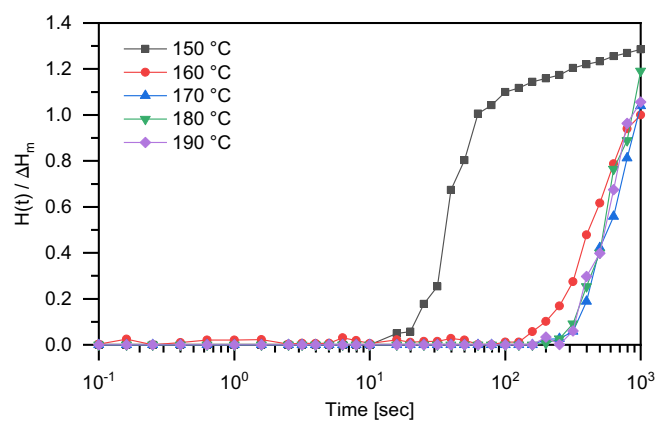

FIGURE 6 Time evolution of crystallinity during the heat treatment process after melting the polymer at five different temperatures. [Color figure can be viewed at wileyonlinelibrary.com]

$$\text{Open cell content}\% = \frac{V_{\text{foam}} - V_{\text{measure}}}{V_{\text{foam}}} \times 100 \quad (3)$$

where V_{foam} is the total volume of the foams, and V_{measure} is the volume of closed cell and polymer volumes measured using a gas pycnometer.

2.9 | Molecular weight evaluation

The average molecular weight and the molecular weight distribution of neat PHBH and foamed PHBH were measured using an HPLC system (CTO-20A, SPD-20A, CBM-20A, LC-20AD, RID-10A, and DGU-20A, Shimadzu Corporation, Japan). Chloroform (Fujifilm Wako Pure Chemical, Japan) was used as an eluent to dilute 0.5 w/v %, and the flow rate was set to 1.0 mL min^{-1}. Polystyrene was used as a standard to calibrate the HPLC elution curve. The number average molecular weight ($\overline{M}_n$), weight average molecular weight ($\overline{M}_w$) and polydispersity index (PDI) ($\overline{M}_w / \overline{M}_n$) were calculated using LC solution software.

3 | RESULTS AND DISCUSSION

3.1 | Rheology and thermal decomposition of molecular weight

Figure 1 shows the frequency sweep rheological test at the five different melting temperatures. The complex viscosity was reduced with increasing measurement temperature. The viscosity reduction became significantly large when the melting temperature increased above 180°C. Furthermore, the slope of G' measured at 190°C was approximately 2, indicating a typical Maxwell viscoelastic polymer. The slope measured below 170°C shows a value less than 2, indicating the residual orientation of chain segments or small crystal fragments, that is, the origin of melt memory.[26,27]

The complex viscosity was reduced with the lowered frequency, as shown in Figure 1c. When the frequency

TABLE 2 Molecular weight of foamed PHBH at different cylinder temperature

Resin	Cylinder temperature °C	Number average $\overline{M}_n$	Weight average $\overline{M}_w$	PDI
PHBH	150	225,739	407,485	1.8
	160	171,818	377,334	2.2
	170	154,562	341,164	2.2
	180	127,513	261,062	2.1
	190	58,132	105,115	1.8

sweep measurement was performed by changing the frequency from 100 to 0.1 rad s^{-1}, it took more than 30 min to complete. It was suspected that thermal decomposition occurred during the measurement. Figure 2 shows the results of the time sweep test at a 10 rad s^{-1} frequency with 0.1% strain. The degree of thermal decomposition at 150°C was not significant. However, it became significant as the melting temperature increased.

3.2 | Crystallization behavior and the melt memory effect

Figure 3 shows the results of the temperature sweep test. The specimen was held at a specified melting temperature before the measurement started. The crystallization temperature was identified where the viscosity increased drastically with decreasing temperature. When the melting temperature was below 170°C, the crystallization temperature appeared at approximately 100°C. On the other hand, when the melting temperature was above 180°C, the crystallization temperature decreased to 60°C. This

phenomenon is known as a melt memory effect, by which self-crystal nucleation is enhanced with the residual crystals.

Figure 4a,b shows the first cooling curve and second heating curve of the PHBH after holding the specimen at the designated melting temperature in the range of 150–190°C. The results confirmed the existence of melt memory, which coincided with the rheological measurement. In the cooling curve obtained after maintaining the melting temperature at 150°C, the crystallization temperature appeared at approximately 120°C. When the melting temperature was maintained below 170°C, the crystallization temperature appeared at approximately 100°C. Holding the melting temperature above 180°C before cooling shifted the crystallization temperature to 60°C.

PHB has a melting point higher than 170°C.[28] Our PHBH contains 94 mol% PHB and 6 mol% PHH. The long side chain of PHH prevents hydrogen bonding between PHB groups and lowers the melting temperature of PHB.[28] PHB forms a crystal phase in PHBH, which most likely gives rise to the melt memory effect: when processing or melting PHBH at a temperature above

Cylinder Temp.[°C] \ Core-back timing [s]	2	4	8	10
150	60°C	38°C	30°C	30°C
160	74°C	42°C	30°C	30°C
170	83°C	50°C	30°C	30°C
180	95°C	60°C	30°C	30°C
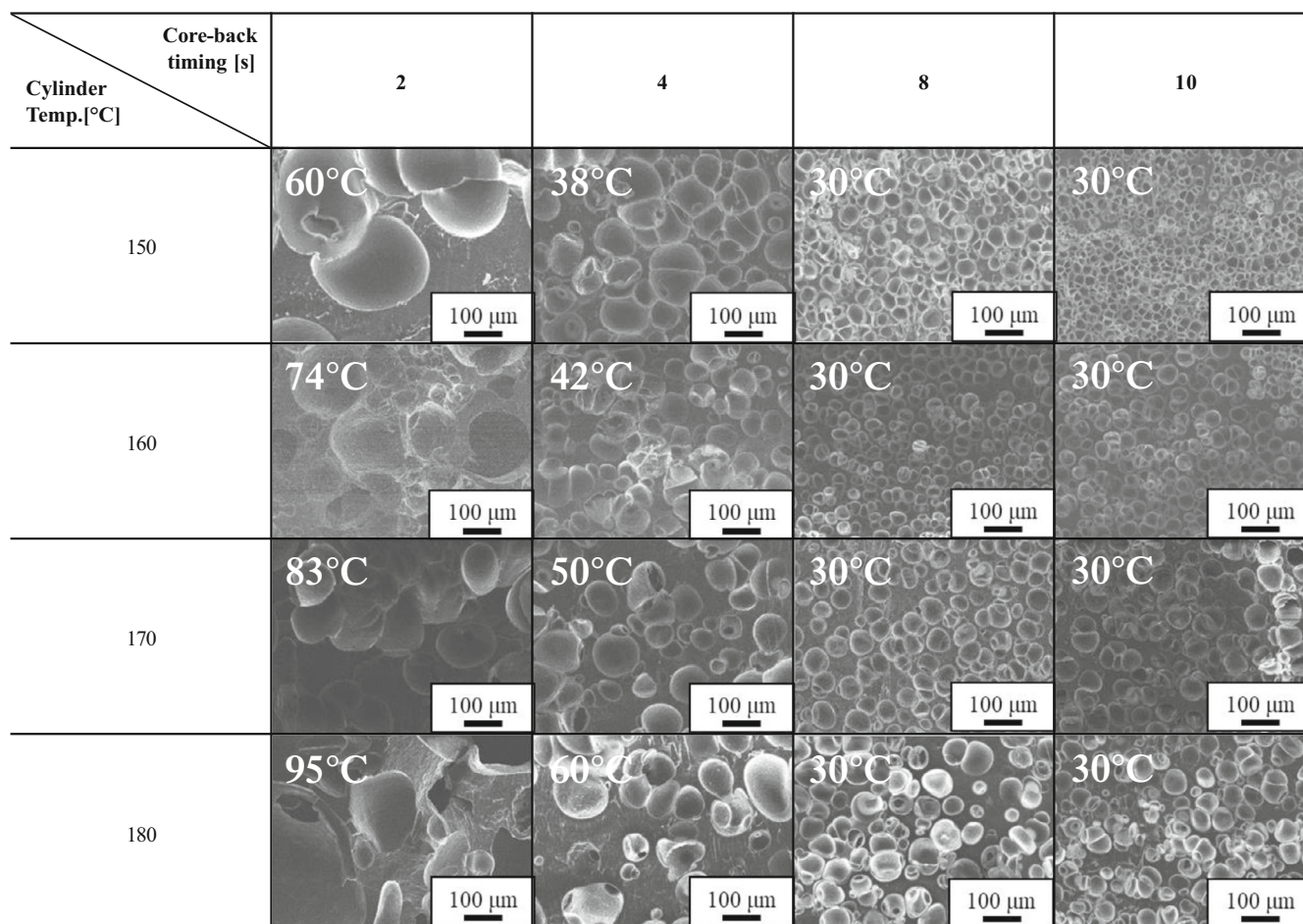
FIGURE 7 SEM images of PHBH foamed at different foaming temperatures and core-back times.

京都大学
KYOTO UNIVERSITY
LEE ET AL.

KURENAI 紅
京都大学学術情報リポジトリ
Kyoto University Research Information Repository

Applied Polymer—WILEY 8 of 11

170°C, the crystals associated with PHB are completely melted. As a result, the crystallization temperature, T_c, becomes 60°C. On the other hand, when melting PHBH at a temperature below 170°C, PHB-associated crystals remain in PHBH and provide crystal nucleation sites. Thus, the crystallization is enhanced, and the crystallization temperature is shifted to 100 from 60°C for the PHBH melted below 170°C. Furthermore, when the melting temperature is 150°C, since it is near the endset of the melting peak, the crystals are not completely melted, resulting in a strong melt memory effect.[29]

Figure 5 shows the polarizing microscope images of the PHBH specimens with approximately the same molecular weight cooled at 40°C after hot pressing at different melting temperatures. The crystal sizes of the specimens with melting temperatures below 160°C were smaller than those with melting temperatures above 170°C This indicates that the melt memory effect was active for the specimens prepared at a melting temperature lower than 170°C.

Figure 6 shows the time evolution of crystallinity during the cooling process after melting the polymer at five different temperatures. The data were acquired by the discrete method of FSC. The crystallization of the specimen melted at 150°C increased rapidly, starting from approximately 10 s, the shortest annealing time. When the melting temperature was above 160°C, crystallization started after 100 s or more. If the melting temperature is 160°C or higher, crystallization begins after 100 s or more. In the rapid cooling process, the FSC showed the
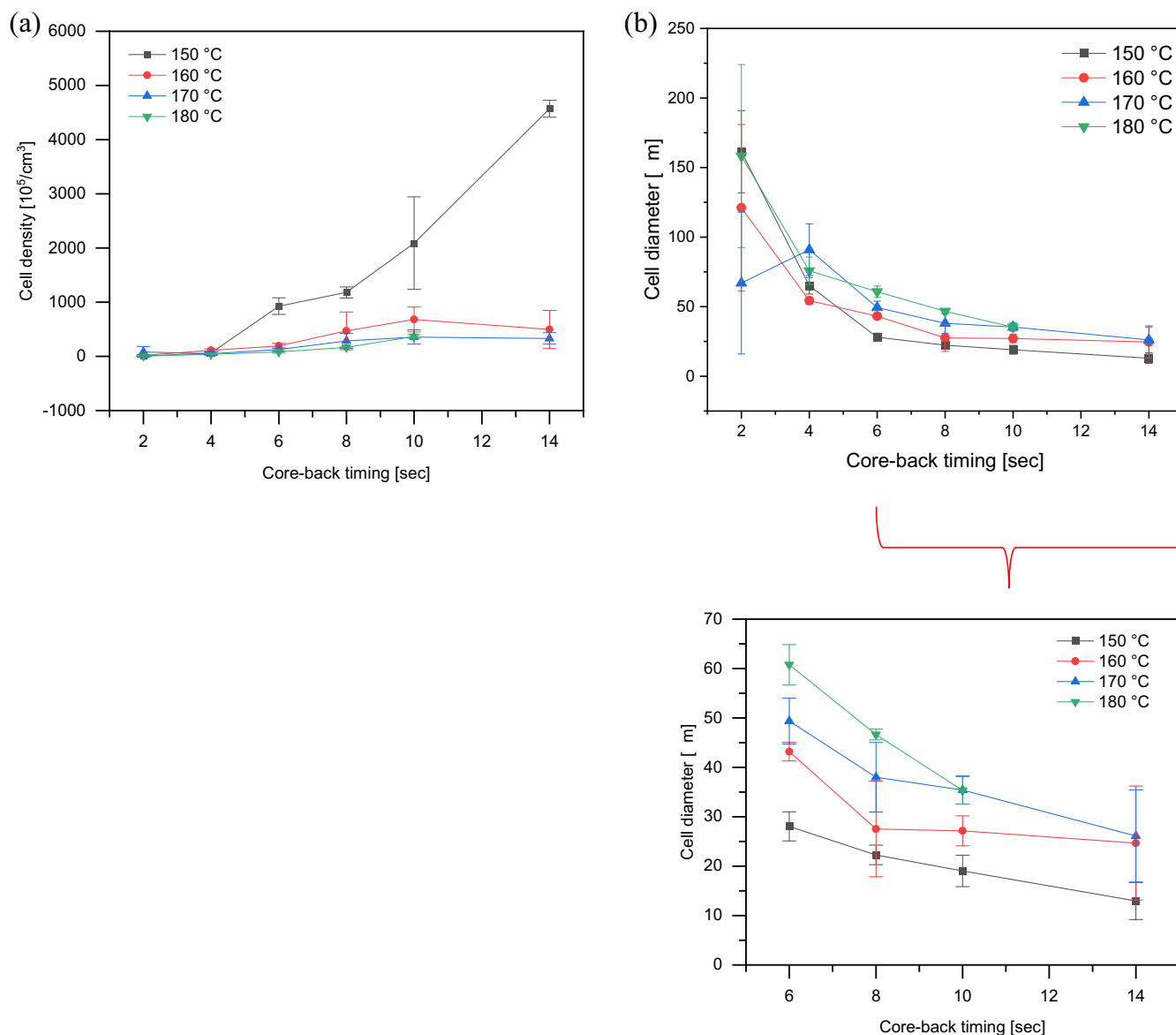

FIGURE 8 (a) Cell density and (b) cell diameter change versus core-back time at the four different melting temperatures. [Color figure can be viewed at wileyonlinelibrary.com]

京都大学
KYOTO UNIVERSITY
9 of 11

JOURNAL OF
WILEY Applied Polymer
SCIENCE

A Self-archived copy in
Kyoto University Research Information Repository
https://repository.kulib.kyoto-u.ac.jp

京都大学学術情報リポジトリ
KURENAI 紅
Kyoto University Research Information Repository

LEE ET AL.

melting memory effect appeared only in the specimens melted at 150°C, a melting temperature lower than that observed in the slow cooling process shown in Figure 4.

The DSC has a relatively slow cooling rate, providing enough time for PHBH to crystallize. However, in the case of the FSC, it is difficult to track the crystallization of a polymer with a slow crystallization rate, such as PHBH, due to a much faster cooling rate than that of the DSC. Therefore, the melting memory effect shown at 150°C measured in the rapid cooling process means that it has a stronger melting memory effect than when melted at 160 or 170°C.

3.3 | Foam injection-molded PHBH and its cell structure

Foam injection molding with five different melting temperatures, 150, 160, 170, 180, and 190°C, was performed while keeping the mold temperature at 30°C. By tuning the core-back timing in the range of 2–14 s, threefold expansion foams were successfully prepared at four different melting temperatures, except 190°C. Thermal degradation occurred during FIM processing, as shown in Table 2. As the melting temperature increased, the decomposition ratio of PHBH and the degree of molecular weight reduction increased. The viscosity of the injected polymer also decreased with the reduced molecular weight and led to larger cells in the foam. The foam could not be obtained from the 190°C processed PHBH because of the lower viscosity, low T_c, and lack of the melt memory effect.

Figure 7 shows SEM images of the cell structure of the PHBH foams prepared at different melting temperatures and core-back timings. The value at the upper left corner of each image indicates the foaming temperature corresponding to the core-back timing. Figure 8 shows the cell density and diameter of the foams prepared at four different melting temperatures and core-back timings. When the core-back operation was conducted between 2 and 4 s, the cell size was large, and the cell density was low regardless of the melting temperature. As the core-back operation was delayed, cooling of the polymer progressed in the mold cavity. Then, the foaming temperature was lowered, and the viscosity was increased. The increased viscosity suppressed cell growth, decreasing the cell size. The effect of core-back timing or foaming temperature was more prominent on the cell density than cell diameter, especially for the foam prepared from the polymer at a 150°C melting temperature. As shown in Figure 8, an exponential increase in cell density was observed for the foams prepared by delaying the core-back time longer than 6 s, and the cell size of the foams became the finest, especially when the core-back time was longer than 10 s. Figure S3 shows the cell size distribution in the foams. The cell structure of the foams prepared at a 150°C melting temperature became narrower, indicating high uniformity. Delaying the core-back operation or lowering the foaming temperature provided more cell nucleation sites to the PHBH injected at a 150°C melting temperature. This is an indication of the effect of melt memory on higher cell density.

3.4 | Mechanical properties

Figure 9a shows the compression S–S curves of PHBH foamed with 10 s of core-back timing. The compressive
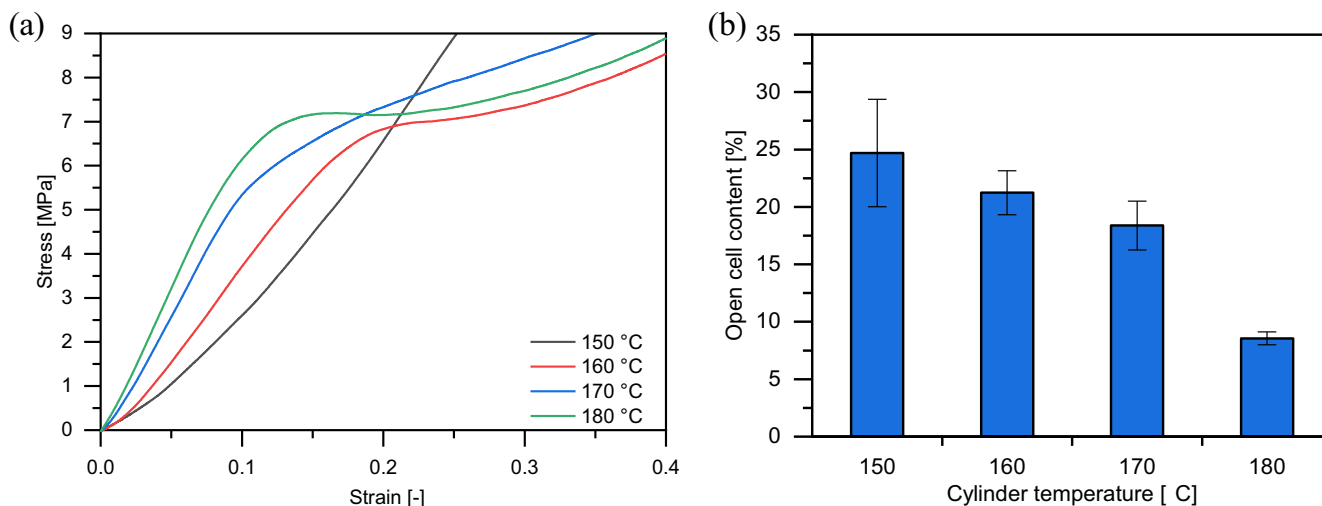

FIGURE 9 (a) S–S curves of foamed PHBH with 10 s of core-back timing and (b) open contents of the foams prepared with different melting temperatures. [Color figure can be viewed at wileyonlinelibrary.com]

京都大学
KYOTO UNIVERSITY
LEE ET AL.

Applied Polymer—WILEY | **10 of 11**

KURENAI 紅
京都大学学術情報リポジトリ
Kyoto University Research Information Repository

stress of the foam prepared at 150°C increased exponentially, and the yield stress point did not appear, indicating high ductility. Because it was manufactured at a low cylinder temperature, thermal decomposition and molecular weight reduction were prevented. Therefore, even when the compressive stress increased, elastic deformation instead of cell rupture continued to occur. On the other hand, foams manufactured at a melting temperature higher than 160°C showed a yield point where structural deformation and cell rupture occurred. Because the ductility decreased due to the molecular weight reduction, structural deformation occurred at the lower compression stress.

Figure 9b shows the open cell content of the foams prepared with different processing temperatures (FIM cylinder temperatures). The open cell content of the sample prepared at 150°C is the highest. The lower the melting temperature is, the smaller the cell size and the higher the open cell content. The open cell content often increases with the decrease in cell size, even when the expansion ratio is the same. The elastic modulus and yield stress usually decrease when the open cell content increases. In other words, the large compression stress produced in the foam manufactured at 150°C could be caused by small crystals produced with melt memory.

4 | CONCLUSION

Because of the weak heat resistance of PHBH, thermal decomposition occurs depending on the processing time and makes polymer processing difficult. Finding an optimal foam injection molding condition for preparing the microcellular foams was challenging. Rheological and thermal analyses were conducted to understand the effect of the melting temperature on the molecular weight and viscosity reduction. The analyses revealed that thermal decomposition could be suppressed when the melting temperature, that is, the injected polymer temperature, was set to 150°C, and the melt memory effect could be maintained by setting the melting temperature below 170°C. When the heat-treatment temperature was below 170°C, the crystallization temperature appeared at approximately 100°C.

On the other hand, when the temperature was above 180°C, the crystallization temperature decreased to 60°C. The microcellular foam could be prepared by using the melt memory effect. The cell density and uniformity of the cellular structure became prominent in the foams prepared with the 150°C melting temperature.

In the case of harsh nonisothermal conditions, such as a very rapid cooling condition of the injection molding process, the melt memory effect works at a lower temperature than that rheological and thermal measurements could identify. In particular, the crystallization temperature, T_c, in the presence of melt memory would shift to a temperature lower than 100°C. Therefore, the optimal melting temperature condition for microcellular foam preparation was lower than 170°C. Through foaming experiments, it was revealed that the melt memory effect could provide cell nucleation sites through the crystals in foams prepared with melting temperatures in the range of 150–160°C. The results of this study could be helpful for manufacturing PHBHs with other processes.

AUTHOR CONTRIBUTIONS

Jisuk Lee: concepualization; data curation; formal analysis; investigation; methodology; navisualization. **Kenta Moriyama:** Formal analysis (supporting); investigation (supporting); methodology (supporting). **Yuta Hikima:** Conceptualization (supporting); investigation (supporting); methodology (supporting). **Masahiro Ohshima:** Conceptualization; projection administration; supervision; writing-revies & editing.

ACKNOWLEDGMENTS

DATA AVAILABILITY STATEMENT

The data that support the findings of this study are available from the corresponding author upon reasonable request.

ORCID

Jisuk Lee https://orcid.org/0000-0002-1743-3852
Masahiro Ohshima https://orcid.org/0000-0003-0870-5438

REFERENCES

[1] C. S. Reddy, R. Ghai, Rashmi, V. Kalia, *Bioresour. Technol.* **2003**, *87*, 137.
[2] M. Mehrpouya, H. Vahabi, M. Barletta, P. Laheurte, V. Langlois, *Mater. Sci. Eng. C* **2021**, *127*, 127.
[3] S. Y. Lee, *Biotechnol. Bioeng.* **2000**, *49*, 1.
[4] T. Watanabe, Y. He, T. Fukuchi, Y. Inoue, *Macromol. Biosci.* **2001**, *1*, 75.
[5] C. Chen, M. K. Cheung, P. H. F. Yu, *Polym. Int.* **2005**, *54*, 1055.
[6] W. Arifin, T. Kuboki, *Polym. Compos.* **2018**, *39*, 491.
[7] J. Zhou, X. Ma, J. Li, L. Zhu, *Cellulose* **2019**, *26*, 979.
[8] N. Hosoda, T. Tsujimoto, H. Uyama, *ACS Sustain. Chem. Eng.* **2014**, *2*, 248.
[9] R. P. Juntunen, V. Kumar, J. E. Weller, W. P. Bezubic, *J. Vinyl Addit. Technol.* **2000**, *6*, 93.
[10] T. Ishikawa, K. Taki, M. Ohshima, *Polym. Eng. Sci.* **2012**, *52*, 875.

[11] L. Wang, S. Ishihara, M. Ando, A. Minato, Y. Hikima, M. Ohshima, *Ind. Eng. Chem. Res.* **2016**, *55*, 11970.

[12] L. Wang, Y. Hikima, S. Ishihara, M. Ohshima, *Polymer (Guildf)* **2017**, *128*, 119.

[13] P. Chen, W. Wang, Y. Wang, K. Yu, H. Zhou, X. Wang, J. Mi, *Polym. Degrad. Stab.* **2017**, *144*, 231.

[14] D. Yin, J. Mi, H. Zhou, X. Wang, K. Yu, *J. Appl. Polym. Sci.* **2020**, *137*, 48850.

[15] J. S. Colton, N. P. Suh, *Polym. Eng. Sci.* **1987**, *27*, 493.

[16] R. Miyamoto, S. Yasuhara, H. Shikuma, M. Ohshima, *Polym. Eng. Sci.* **2014**, *54*, 2075.

[17] L. Sangroniz, A. Sangroniz, L. Meabe, A. Basterretxea, H. Sardon, D. Cavallo, A. J. Müller, *Macromolecules* **2020**, *53*, 4874.

[18] A. T. Lorenzo, M. L. Arnal, J. J. Sánchez, A. J. Müller, *J. Polym. Sci. B Polym. Phys.* **2006**, *44*, 1738.

[19] X. Chen, C. Qu, R. G. Alamo, *Polym. Int.* **2019**, *68*, 248.

[20] X. Liu, Y. Wang, Z. Wang, D. Cavallo, A. J. Müller, P. Zhu, Y. Zhao, X. Dong, D. Wang, *Polymer (Guildf)* **2020**, *188*, 122117.

[21] J. Rault, *Crit. Rev. Solid State Mater. Sci.* **1986**, *13*, 57.

[22] M. Kutz, *Applied Plastics Engineering Handbook: Processing and Materials* (Ed: M. Kutz), William Andrew, Waltham, USA **2011**.

[23] R. Gendron, *Thermoplastic Foam Processing: Principles and Development* (Ed: R. Gendron), CRC Press, Boca Raton **2004**.

[24] G. Wang, G. Zhao, S. Wang, L. Zhang, C. B. Park, *J. Mater. Chem. C* **2018**, *6*, 6847.

[25] X. Tardif, B. Pignon, N. Boyard, J. W. P. Schmelzer, V. Sobotka, D. Delaunay, C. Schick, *Polym. Test.* **2014**, *36*, 10.

[26] A. Ito, T. Semba, K. Kitagawa, H. Okumura, H. Yano, *J. Cell. Plast.* **2019**, *55*, 385.

[27] V. Khoshkava, M. R. Kamal, *ACS Appl. Mater. Interfaces* **2014**, *6*, 8146.

[28] H. Sato, Y. Ando, H. Mitomo, Y. Ozaki, *Macromolecules* **2011**, *44*, 2829.

[29] T. Aoyama, H. Sato, Y. Ozaki, *Polym. Cryst.* **2019**, *2*, 1.

SUPPORTING INFORMATION

Additional supporting information can be found online in the Supporting Information section at the end of this article.